Article

Atomic Scale Insights on Chlorinated #-Alumina Surfaces

Mathieu Digne, Pascal Raybaud, Philippe Sautet, Denis Guillaume, and Herve# Toulhoat

J. Am. Chem. Soc., **2008**, 130 (33), 11030-11039 • DOI: 10.1021/ja8019593 • Publication Date (Web): 23 July 2008

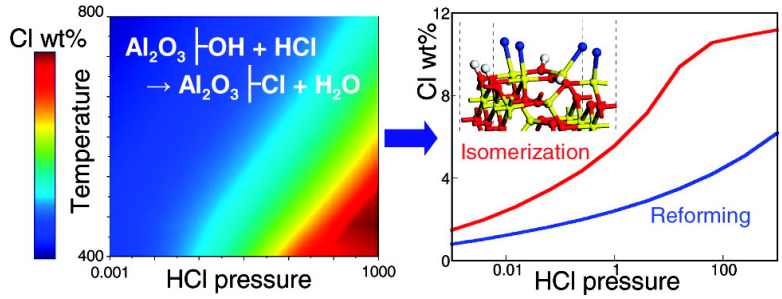

More About This Article

Additional resources and features associated with this article are available within the HTML version:

- Supporting Information
- Access to high resolution figures
- Links to articles and content related to this article
- Copyright permission to reproduce figures and/or text from this article

View the Full Text HTML

J|A|C|S
ARTICLES

Published on Web 07/23/2008

Atomic Scale Insights on Chlorinated γ-Alumina Surfaces

Mathieu Digne,[†] Pascal Raybaud,[*,‡] Philippe Sautet,[§] Denis Guillaume,[‡] and Hervé Toulhoat[⊥]

Direction Physique et Analyse, Direction Catalyse et Séparation, IFP, Rond-point de l'échangeur de Solaize, BP 3, 69390 Solaize, France, Université de Lyon, Institut de Chimie, Laboratoire de Chimie, Ecole normale supérieure de Lyon, CNRS 46, allée d'Italie, 69364 Lyon cedex 07, France, and Direction Scientifique, IFP, 1-4 avenue de Bois-Préau, 92852 Rueil-Malmaison cedex, France

Received March 17, 2008; E-mail: pascal.raybaud@ifp.fr

Abstract: The thermochemistry of chlorinated γ-alumina surfaces is explored by means of density functional calculations as a function of relevant reaction conditions used in experiments and in high-octane fuel production in the refining industry such as hydrocarbon isomerization and reforming. The role of chlorine as a dope of the Brønsted acidity of γ-alumina surfaces is investigated at an atomic scale. Combining infrared spectroscopy and density functional theory calculations, the most favorable location of chlorine atoms on the (110), (100) and (111) surfaces of γ-alumina is found to result either from direct adsorption or from the exchange of basic hydroxyl groups. Moreover, the modification of the hydrogen bond network upon chlorine adsorption is put forward as a key parameter for changing the Brønsted acidity. In a second step, we use a thermodynamic approach based on DFT total energy calculations corrected by the chemical potentials of HCl and H_2O to determine the adsorption isotherms of chlorine and the relative surface concentration of hydroxyl groups and chlorine species on the γ-alumina surfaces. The determination of chlorine content as a function of temperature and partial pressures of H_2O and HCl offers new quantitative data required for optimizing the state of the support surface in industrial conditions. The mechanisms of chlorination are also discussed as a function of reaction conditions.

Introduction

The metastable γ-polymorph of alumina (γ-Al_2O_3) is an important oxide material used as the support of numerous catalytic active phases such as metals or transition metal sulfides. From the mesoscale to the nanoscale, γ-Al_2O_3 exhibits very versatile physical chemical properties[1] required for refining catalytic processes, such as hydrotreatment to reduce the sulfur content of diesel,[2] or naphtha reforming or isomerization to increase the gasoline octane number.[3,4] Moreover, the naphtha reforming process involving dehydrogenation reactions of alcanes and naphtenes is also the main source of hydrogen in refineries. The hydrogen balance will remain an increasing concern of refiners within the context of biofuels production or coal liquids refining, which need higher consumption of H_2 for reducing the oxygen content. As a consequence, the improvement of the γ-Al_2O_3 properties is at the core of many future challenges for the refining, petrochemical, and energy industry.

At the mesoscale, the high specific area of the γ-Al_2O_3 support (usually around 200 m^2 per gram) favors the high dispersion degree of the active-phase crystallites exhibiting nanometer sizes or even less, as for reforming catalysts where the metallic active phase is made of small clusters for which the Pt−Pt coordination number measured by X-ray absorption spectroscopy (XAFS) is less than 7.[5,6] At the atomic scale, the acidic−basic properties of the oxide support can directly be involved during the catalytic reactions. Again, a relevant example is highlighted by bifunctional reforming catalysts such as γ-alumina-supported bimetallic PtX bimetallic (X = Re, Ir, or Sn). The (de)hydrogenation and hydrogenolysis reactions are taking place on the metallic active phase, whereas the acidic properties of the support enhance the cracking and isomerization reactions.[4,5] For these reasons, understanding how to control the acidic−basic properties of the support's surfaces at the atomic scale is a challenging fundamental scientific issue with practical industrial applications. In the case of industrial reforming and isomerization catalysts, the surface acidity of γ-Al_2O_3 is modified by adsorbing halogens (such as Cl or F) on the surface. A large number of modifying agents have been tested for different catalytic applications, even if chlorine remains one of the most widely used dopes to modify the surface

[†] Direction Physique et Analyse, IFP.
[‡] Direction Catalyse et Séparation, IFP.
[§] Université de Lyon, Institut de Chimie.
[⊥] Direction Scientifique, IFP.

(1) Euzen, P.; Raybaud, P.; Krokidis, X.; Toulhoat, H.; Loarer, J.-L. L.; Jolivet, J.-P.; Froidefond, C. In *Handbook of Porous Solids*; Schüth, F., Sing, K. S. W., Weitkamp, J., Eds.; Wiley-VCH Verlag GmbH: Weinheim, 2002; Vol. 3.
(2) Prins, R. In *Handbook of Heterogeneous Catalysis*; Ertl, G., Knözinger, H., Weitkamp, J., Eds.; Wiley-VCH Verlag GmbH: Weinheim, 1997; Vol. 4.
(3) Ertl, G., Knözinger, H., Weitkamp, J., Eds. *The Handbook of Heterogeneous Catalysis*; Wiley-VCH: Weinheim, 1997.
(4) Marcilly, C. *Acid-Base Catalysis: Application to Refining and Petrochemistry*; Edition Technip: Paris, 2005; Vol. 2, Chapter 10.
(5) Sinfelt, J. H. In *Handbook of Heterogeneous Catalysis*; Ertl, G., Knözinger, H., Weitkamp, J., Eds.; Wiley-VCH: Weinheim, 1997; Vol. 3, Chapter 3.9.
(6) Lynch, J. *Oil Gas Sci. Technol.* **2002**, *57*, 281.

10.1021/ja8019593 CCC: $40.75

acidity. For instance, the chlorination of alumina is used to improve alkylation[7] or cracking[8] reactions. The chlorination of the γ-alumina surfaces is accomplished by the use of various chlorinating agents (HCl, CCl_4, or $AlCl_3$). The quantity of chlorine fixed and the resulting acidity depend on the chlorinating agents and of the reaction conditions (temperature, partial pressure of chlorinating agents, and water) used for the chlorination. For reforming, the quantity of chlorine added is about 1−2 wt %, whereas for isomerization, the chlorine content may reach 6−7 wt %. The chlorination occurs always by chemical exchange of the surface hydroxyl (−OH) groups.[4,9] Since this exchange is reversible, the chemical potential of water in the reaction environment must be controlled because an excess of water could be detrimental to the stability of chlorine at the surface. In addition, it is also known that the chlorine addition may prevent the sintering of metallic clusters by ensuring high dispersion state and low Pt−Pt coordination number.[6] In industrial conditions, to maintain this high dispersion state, the catalyst is continuously regenerated under a chlorinated atmosphere. Moreover, depending on the chlorine content of the catalyst's support, this coordination number may reach values below 4.[6,10] Moreover, XAFS studies seem to indicate that the nature of the support may modify the electronic features of small Pt clusters[11] and, as a result, the hydrogen adsorption property of those clusters.[12] Recent density functional theory (DFT) studies have underlined the role of the hydration state of the γ-alumina surfaces on the adsorption and diffusion properties of Pd_n ($1 \leq n \leq 5$) clusters.[13,14] The hydration state influences the distribution of hydroxyl (−OH) groups and Lewis acid aluminum sites. In particular, it has been shown that the adsorption mode of ethylene on γ-alumina-supported Pd_4 clusters depends on the hydroxylation state of the γ-alumina surfaces.[15] As a consequence, further improvements of metallic active phases highly dispersed on doped γ-alumina surfaces are expected to be directly linked with deeper understanding of the nano- and atomic-scale properties of the doped surfaces. A challenging question concerns the role of the hydroxylation state and crystallographic orientation of the γ-alumina surfaces when doped by anionic and cationic species. However, the use of small $Pt_4/(X_2O)_3$ clusters (X = F, H, Na) as proposed in refs 12 and 16 cannot be fully satisfactory to describe the surface state of the support. This approach may raise questions about the overestimate of the effect of the X_2O ligand and the simultaneous underestimate of surface rearrangements which modify the nature of the chemical interactions between Pt clusters and the doped γ-alumina surfaces. In contrast, recent periodic DFT calculations have brought many relevant insights about the bulk[17–19] and surface properties [20–22] of γ-alumina under realistic environment. In particular, the effect of various reaction conditions such as temperature, partial pressures of reactants (such as H_2O, H_2S, H_2) [20,21,23–25] were included to determine the precise surface state of γ-alumina. More recently, we have also proposed a rational model based on DFT calculations and infrared (IR) characterization to explain the poisoning of the γ-alumina surface acidity by the sodium cation.[26] In particular, Na cations were found to be located in an inner sphere complex of surface hydroxyls and oxygen atoms after exchanging protons from surface μ_3-OH groups. This model's chemistry significantly differs from that of the cluster model used in reference 12. However, even if the adsorption of HCl molecules on ideal dehydrated α-alumina (0001) surface has been investigated by periodic DFT simulation,[27] the challenging study of chlorinated γ-alumina surface remained to be undertaken.

According to the crucial role of chlorine as surface modifier of γ-alumina properties, the determination of reliable surface models of chlorinated γ-alumina is an important question. In the context of reforming, the balance between H_2O and HCl is known to be critical for optimizing the physical chemical properties of the metallic active phase. In this paper, we thus propose to use density functional theory (DFT) and infrared (IR) analysis of chlorinated γ-alumina nanocrystalline samples synthesized in well-defined conditions in order to build realistic theoretical models of chlorinated γ-Al_2O_3 surfaces for various chlorine coverages. First the stable location of the chlorine elements on the surface is determined, and the impact of the surface OH stretching frequencies is discussed with respect to the IR experimental results. The influence of chlorine on surface acidity is also studied by means of pyridine adsorption calculations. Then, a thermodynamic model is proposed in combination with DFT results to determine the domains of stability of hydroxyl and chlorine species at the surface. Finally, the calculation of chlorine contents of the γ-alumina surface as a function of temperature and the partial pressures of H_2O and HCl is presented. It is shown how this model is expected to find practical applications in the reforming and isomerization processes, where these parameters are fixed in order to control the catalytic surface state.

Theoretical Methods

Total Energy Calculation. The computational method used for total energy calculation is coherent with the one used in our previous published works where the hydroxylated surfaces

(7) Clet, G.; Goupil, J. M.; Szabo, G.; Cornet, D. *J. Mol. Catal. A: Chem.* **1999**, *148*, 253.
(8) Guillaume, D.; Gautier, S.; Alario, F.; Devès, J. M. *Oil Gas Sci. Technol.* **1997**, *54* (4), 537.
(9) Gates, B. C.; Katzer, J. R.; Schuit, G. C. A. *Chemistry of Catalytic Processes*; McGraw-Hill: New York, 1979.
(10) Berdala, J.; Freund, E.; Lynch, J. P. *J. Phys. (Paris)* **1986**, *47*, C8–269.
(11) Ramaker, D. E.; Oudenhuijzen, M. K.; Koningsberger, D. C. *J. Phys. Chem. B* **2005**, *109*, 5608.
(12) Oudenhuijzen, M. K.; Bokhoven, J. A. v.; Miller, J. T.; Ramaker, D. E.; Koningsberger, D. C. *J. Am. Chem. Soc.* **2005**, *127*, 1530.
(13) Valero, M. C.; Raybaud, P.; Sautet, P. *J. Phys. Chem. B* **2006**, *110*, 1759.
(14) Valero, M. C.; Raybaud, P.; Sautet, P. *Phys. Rev. B* **2007**, 045427.
(15) Valero, M. C.; Raybaud, P.; Sautet, P. *J. Catal.* **2007**, *247*, 339.
(16) Thomson, J.; Webb, G.; Webster, B. C.; Winfield, J. M. *J. Chem. Soc., Faraday Trans.* **1995**, *91*, 155.
(17) Krokidis, X.; Raybaud, P.; Gobichon, A.-E.; Rebours, B.; Euzen, P.; Toulhoat, H. *J. Phys. Chem. B* **2001**, *105*, 5121.
(18) Wolverton, C.; Haas, K. C. *Phys. Rev. B* **2001**, *63*, 024102.
(19) Paglia, G.; Buckley, C. E.; Rohl, A. L.; Hunter, B. A.; Hart, R. D.; Hanna, J. V.; Byrne, L. T. *Phys. Rev. B* **2003**, *68*, 144110.
(20) Digne, M.; Sautet, P.; Raybaud, P.; Euzen, P.; Toulhoat, H. *J. Catal.* **2002**, *211*, 1.
(21) Digne, M.; Sautet, P.; Raybaud, P.; Euzen, P.; Toulhoat, H. *J. Catal.* **2004**, *226*, 54.
(22) Valero, M. C.; Digne, M.; Sautet, P.; Raybaud, P. *Oil Gas Sci. Technol.* **2006**, *61*, 535.
(23) Arrouvel, C.; Digne, M.; Breysse, M.; Toulhoat, H.; Raybaud, P. *J. Catal.* **2004**, *222*, 152.
(24) Arrouvel, C.; Breysse, M.; Toulhoat, H.; Raybaud, P. *J. Catal.* **2004**, *226*, 260.
(25) Joubert, J.; Fleurat-Lessard, P.; Delbecq, F.; Sautet, P. *J. Phys. Chem. B* **2006**, *110*, 7392.
(26) Digne, M.; Raybaud, P.; Sautet, P.; Guillaume, D.; Toulhoat, H. *Phys. Chem. Chem. Phys.* **2007**, *9*, 2577.
(27) Alavi, S.; Sorescu, D. C.; Thompson, D. L. *J. Phys. Chem. B* **2003**, *107*, 186.

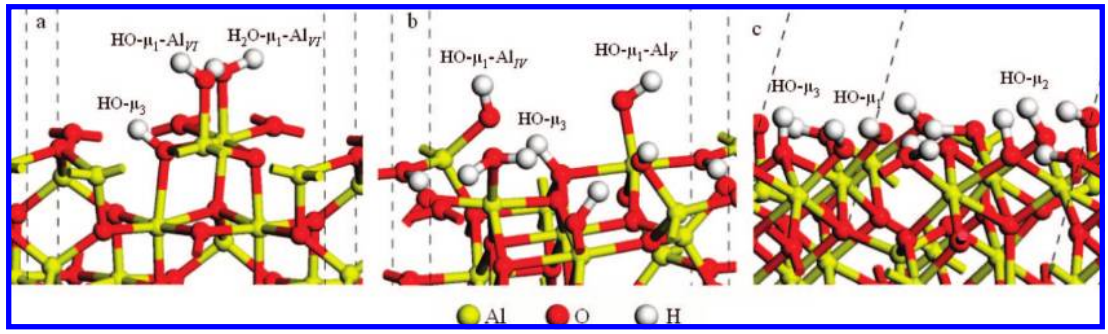

Figure 1. Local structures of the hydroxylated γ-alumina surfaces: (a) γ-Al_2O_3(100) with $\theta_{OH} = 8.8$ OH·nm^{-2} and (b) γ-Al_2O_3(110) with $\theta_{OH} = 11.8$ OH·nm^{-2}; (c) γ-Al_2O_3(111) with $\theta_{OH} = 14.7$ OH·nm^{-2} in absence of chlorine. The most relevant surface OH groups are labeled: Al_X stands for aluminum atoms surrounded by X oxygen atoms and HO-μ_n for OH groups linked to n aluminum atoms.

Table 1. Substitution of the Surface Hydroxyl Groups by Chlorine: Effect of the Local Environment

site	surface	ω_{calc} (cm^{-1})	$\Delta_r E$ (kJ·mol^{-1})
HO-μ_1-AI_{IV}	(110)	3842	+19
HO-μ_1-Al_{VI}	(100)	3777	+2
HO-μ_1-Al_V	(110)	3736	−4
HO-μ_2-Al_{VI}	(110)	3707	+29
HO-μ_3-Al_{VI}	(100)	3589	+95
HO-μ_1-Al_{IV} (H-bonded)	(110)	3206	+42
H_2O-μ_1-Al_V	(110)	3717	+31
H_2O-μ_1-Al_{VI}	(100)	3616	+12
HO-μ_3-Al_{VI}	(111)	3752	+119
HO-μ_2-Al_{VI}	(111)	3732	+58
HO-μ_1-Al_{VI}	(111)	3712	+26

of non doped γ-alumina surface were determined.[20,21] The calculations are based on density functional theory (DFT), as implemented in the Vienna Ab initio Simulation Package (VASP),[28,29] with the Perdew−Wang 91 (PW91) generalized gradient-corrected exchange-correlation functional.[30,31] Ultrasoft pseudopotentials are used for each atom. Periodic boundary conditions are set, leading to an infinite periodically repeated system. The wave functions of the Kohn−Sham Hamiltonian are expanded on a plane wave basis set with an energy cutoff of 300 eV. For each atomic configuration, atomic forces are calculated via the Hellmann−Feynman theorem, and the geometry optimization is performed with a conjugate-gradient algorithm.

Surface Models. The (*hkl*) surfaces, simulated using a slab model, are generated with a least eight atomic layers in the (*hkl*) direction. A vacuum of 12 Å is set between two periodically repeated slabs. Each slab is kept symmetric to avoid unphysical dipolar interaction between two consecutive slabs. In this study, we focus on the three preferentially exposed surfaces of γ-alumina in working conditions: the (100), (110), and (111) surfaces which were identified by neutron diffraction analysis and electron microscopy.[32,33] Our previous DFT works have shown that the hydroxyl concentration at the surfaces depends on temperature and the partial pressure of water.[21,23] According to the temperatures exposed during chlorine exchange and infrared experiments (*vide infra*), the surfaces may exhibit hydroxyl coverages as high as 8.8 OH·nm^{-2} on the (100) surface, 11.8 OH·nm^{-2} on the (110) surface and 14.7 OH·nm^{-2} on the (111) surface as shown in Figure 1.

Thermochemistry of Chlorinated Surfaces. For low chlorine content, a first approach to study the chlorine effect is to assume that the total surface coverage ($\theta_{H_2O} + \theta_{HCl}$) remains constant during chlorination (this assumption will be discussed in detail in the Results section). The surface coverage depends on the experimental conditions: temperature and partial pressures of water and hydrogen chloride. According to the slab supercells used and presented in Figure 1, the substitution of a single OH group increases the chlorine coverage, θ_{HCl}, by 1 to 2 Cl·nm^{-2}.

On the basis of this assumption, the substitution of the different surfaces hydroxyl groups has been considered:

$$-Al_n(OH)- + HCl_{gas} \rightarrow -Al_{n'}(Cl)- + H_2O_{gas} \quad (1)$$

where n (respectively, n') indicates the coordination numbers of the surface OH (respectively, Cl) species.

The total energy balance of reaction 1 can be written as follows:

$$\Delta E_{exch} = E(-Al_{n'}(Cl)-) + E(H_2O) - E(-Al_{n'}(OH)-) - E(HCl) \quad (2)$$

Considering the fact that the entropy contributions of the H_2O and HCl molecules are very close over a wide range of temperatures,[34] the total energy variation as calculated by eq 2 is a first reasonable approximation to evaluate the thermodynamic affinity of chlorine for exchanging different surface OH groups.

For higher chlorine contents depending on the relative partial pressures of H_2O and HCl, a more complex thermodynamic model must be proposed. The stabilization energy is first calculated with respect to the reference energy, E(surf), of the fully dehydrated and dechlorinated surface used as reference:

$$E_{stab} = E(\text{surf} + n_{H_2O}H_2O + n_{HCl}HCl) - E(\text{surf}) - n_{H_2O}E(H_2O) - n_{HCl}E(HCl) \quad (3)$$

where $E(\text{surf} + n_{H_2O}H_2O + n_{HCl}HCl)$ is the total energy of the surface with n_{H_2O} (respectively, n_{HCl}) molecules of H_2O (respectively, HCl) adsorbed.

The adsorption and coadsorption energies of H_2O and HCl for different hydroxyl and chlorine coverage are thus systematically calculated by eq 3. Then, to investigate the thermochemistry of chlorinated γ-alumina surfaces, the effects of entropies,

(28) Kresse, G.; Furthmüller, J. *Phys. Rev. B* **1996**, *54*, 11169.
(29) Kresse, G.; Furthmüller, J. *Comput. Mater. Sci.* **1996**, *6*, 15.
(30) Perdew, J. P.; Wang, Y. *Phys. Rev. B* **1992**, *45*, 13244.
(31) Perdew, J. P.; Chevary, J. A.; Vosko, S. H.; Jackson, K. A.; Pederson, M. R.; Singh, D. J.; Fiolhais, C. *Phys. Rev. B* **1992**, *46*, 6671.
(32) Beaufils, J. P.; Barbaux, Y. *J. Chim. Phys.* **1981**, *78*, 347.
(33) Nortier, P.; Fourre, P.; Saad, A. B. M.; Saur, O.; Lavalley, J.-C. *Appl. Catal.* **1990**, *61*, 141.
(34) Lide, D. R., Ed. *Handbook of Chemistry and Physics*; CRC Press: New York, 1995.

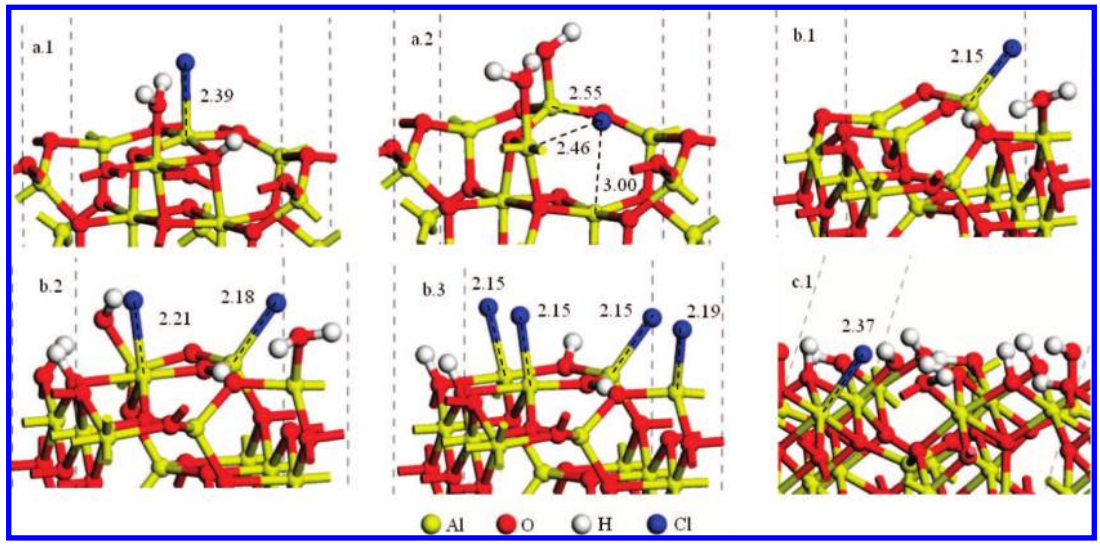

Figure 2. Local structures of chlorinated γ-alumina surfaces: (a) γ-Al_2O_3(100) for 2.15 Cl·nm^{-2} and 6.45 OH·nm^{-2} with Cl in μ_1 position (a.1) and in μ_3 position (a.2), (b) γ-Al_2O_3(110) for different chlorine and hydroxyl contents: (b.1) 1.5 Cl·nm^{-2} and 4.5 OH·nm^{-2}, (b.2) 3.0 Cl·nm^{-2} and 8.9 OH·nm^{-2}, (b.3) 5.9 Cl·nm^{-2} and 5.9 OH·nm^{-2}, (c.1) γ-Al_2O_3(111) for 1.2 Cl·nm^{-2} and 13.5 OH·nm^{-2} (Al−Cl distances are quoted in Å).

temperature, and partial pressures found in the working conditions must be added. For that purpose, we use the following thermodynamic model including the chemical potential of H_2O and HCl molecules in gas phase.

$$G_{stab}(n_{H_2O},n_{HCl}) = E_{stab}(n_{H_2O},n_{HCl}) - n_{H_2O}\mu_{H_2O} - n_{HCl}\mu_{HCl} \quad (4)$$

where

$$\mu_{H_2O}(T,p_{H_2O}) = h^0_{H_2O} - Ts_{H_2O}(T) + RT\ln(p_{H_2O}/p_0) \quad (5)$$

An analogous expression for the chemical potential of HCl is used.

In the Results section, the number of adsorbed molecules will be normalized by surface area, resulting in coverage values.

Theoretical Characterization of Hydroxyl Group Acidity. To evaluate the intrinsic Brønsted acidity of OH groups on the chlorinated surface, the stretching frequencies of OH groups are calculated, using an harmonic approach. The Hessian matrix is calculated by a numerical finite-difference method: each ion is displaced of 0.005 Å around its equilibrium position, in the three directions of space. Due to the high anharmonicity of OH bonds, these harmonic values are corrected by an anharmonicity correction term of 80 cm^{-1} as calculated for similar OH groups of boehmite γ-AlOOH.[35]

Furthermore the adsorption energy of the pyridine molecule was calculated to further characterize the Brønsted acidity of the chlorinated surface by means of the following relationships:

$$\Delta E_{ads} = E(\text{surf} + \text{pyridine}) - E(\text{surf}) - E(\text{pyridine}) \quad (6)$$

where E(surf) is the total energies of the surface, E(pyridine) of the isolated gas-phase pyridine, and E(surf + pyridine) of the adsorbed molecule on the surface. A negative value, corresponding to an exothermic process, indicates an energetically favored adsorption process.

Experimental Section

Preparation of Chlorinated γ-Alumina. The starting material was a γ-Al_2O_3 sample from Axens with a specific surface area of 193 m^2·g^{-1}. Prior to additivation, the sample was calcined at 803 K under flowing dry air for 2 h. Chlorination was performed by submitting the sample to a H_2O−HCl−air stream at 773 K for 2 h. HCl is obtained by the *in situ* decomposition of 1,2-dichloropropane in air, leading to CO_2, H_2O, and HCl. After a calcination at 773 K for 2 h, chlorine content, determined by X-ray fluorescence, was 1.43 wt %. It was thus possible to control the chlorine content at the calcination stage by an atmosphere containing water and chlorinating agents as also observed by others [36,37] following the chemical process represented by the direct equation (1). A similar operation (called oxychloration) is used to regenerate the industrial catalyst.

Next, a partial dechlorination of the support was performed by calcining the sample at 803 K under air with about 20.000 wt ppm of H_2O. By varying the time of calcinations, γ-Al_2O_3 with 1.14 and 0.85 wt % of chlorine, were obtained according to the reverse equation (2).

Infrared (IR) Spectroscopy. Fourier transform infrared spectroscopy has been performed using Digilab TTS80 spectrometer. Samples were used as self-supporting wafers of 20 mg, activated in situ 2 h under vacuum of 10^{-6} mbar at 773 K. Spectra were recorded at room temperature with a resolution of 4 cm^{-1}, and the number of scans was fixed to 300.

Results and Discussion

Low Chlorine Coverages. The enthalpy variation, associated to eq 1, is reported in Table 1. The optimized structures for the most relevant configurations after chlorine exchange are reported in Figure 2. In most cases, the substitution of OH by Cl is an endothermic process. The general trend can be resumed as follows, whatever the crystallographic planes considered. (i) The substitution of the μ_3-OH and μ_2-OH groups is a endothermic process (from +29 to +119 kJ·mol^{-1}), (ii) the substitution of the μ_1-OH groups is an athermic or slightly endothermic process (from −4 to +36 kJ·mol^{-1}), (iii) the existence of hydrogen bonds tends to destabilize the substitution by chlorine atoms, and (iv) the substitution of chemisorbed water molecules is slightly endothermic and leads to the dissociation of the HCl molecule.

(35) Raybaud, P.; Digne, M.; Iftmie, R.; Wellens, W.; Euzen, P.; Toulhoat, H. *J. Catal.* **2001**, *201*, 236.
(36) Castro, A. A.; Scelza, O. A.; Benvenuto, E. R.; Baronetti, G. T.; Parera, J. M. *J. Catal.* **1981**, *69*, 222.
(37) Castro, A. A.; Scelza, O. A.; Baronetti, G. T.; Fritzler, M.; Parera, J. M. *Appl. Catal.* **1983**, *6*, 347.

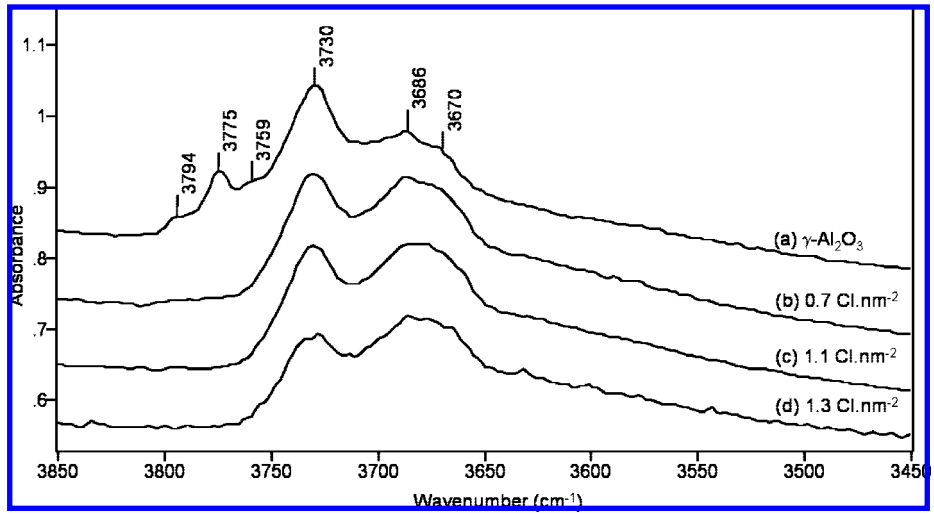

Figure 3. Effect of chlorine content on the high-frequency region of the IR spectrum. A pure γ-alumina sample is compared to samples with increasing chlorine content.

Results (i) and (ii) can be explained by the differences between the optimal distances for Al−OH bonds (1.8−2.0 Å) and for Al−Cl bonds (2.2−2.4 Å). For a μ_1 species, a single distance has to be optimized: the Cl atom relaxes on the surface in order to match the optimal Al−Cl distance (for instance, 2.39 Å for the Al_{VI}-μ_1 group of the (100) surface, Figure 2 a.1). For the μ_2 and μ_3 groups, two or three Al−Cl have to be optimized, the aluminum atoms remaining mainly fixed due the alumina network. The geometrical optimization leads to strong local deformations, energetically unfavorable (Figure 2 a.2). The impact of the hydrogen bond network on the substitution enthalpy is due to the fact that the O−H···Cl hydrogen bond is weaker than the O−H···OH bond. As a consequence, the substitution of a hydrogen bond involving OH groups (donor or acceptor) is more difficult than the substitution of a similar OH group without hydrogen bonds. This effect is well illustrated by the (111) surface, which exhibits a high hydroxyl coverage (14.7 OH·nm^{-2}) and a high density of hydrogen bonds: the substitution is always more endothermic, compared to the less hydroxylated (100) and (111) (+119 kJ·mol^{-1} for the (111) HO-μ_3-Al_{VI} compared to +95 for the (100) HO-μ_3-Al_{VI}, +58 kJ·mol^{-1} for the (111) HO-μ_2-Al_{VI} compared to +29 for the (110) HO-μ_2-Al_{VI},...).

This part of our study provides an accurate localization of the chlorine on the γ-alumina surfaces. Chlorine atoms form surface Cl-μ_1-Al groups in substitution of HO-μ_1-Al groups. Moreover, the presence of strong hydrogen-bond networks (as found on the (111) surface) makes the Cl substitution energetically less favorable.

Vibrational Spectroscopy Analysis. The infrared spectra of pure γ-alumina exhibits five high-frequency bands 3794, 3775, 3730, 3686, and 3670 cm^{-1} corresponding to the OH stretching frequencies (Figure 3 a). According to our previous ab initio simulations carried out,[21] these bands have been assigned to (110) HO-μ_1-Al_{IV}, (100) HO-μ_1-Al_{VI}, (110) HO-μ_1-Al_V, HO-μ_2, and HO-μ_3. Numerous examples illustrating the parallel between IR experiments and DFT simulations can be found in a recent review.[38] In what follows, we focus on the impact of chlorine on this high-frequency region. The introduction of 0.7 Cl·nm^{-2} leads to the total disappearance of the bands located at 3794 and 3775 cm^{-1}. Increasing the Cl coverage, the intensity of the band at 3730 cm^{-1} is decreasing, relative to the intensity of HO-μ_2 and HO-μ_3 bands. Using the previous calculations of chlorine exchange, the interpretation of these experimental observations is straightforward. At very low chlorine content (around 1 Cl·nm^{-2}), the first OH species involved in the exchange are preferentially the (110) HO-μ_1-Al_{IV}, the (110) HO-μ_1-Al_V, and the (100) HO-μ_1-Al_{VI} groups. From a pure spectroscopic analysis of OH stretching bond, these groups are considered as the most basic ones, being also intrinsically the most labile. The corresponding frequencies of these groups thus disappear from the spectra. At the same time, the bands assigned to the HO-μ_2 and HO-μ_3 groups are only slightly modified by chlorine addition. A broadening of these bands is noticed for the higher chlorine content. We propose the following explanation of this broadening by the fact that on hydroxylated surfaces, some OH groups are hydrogen bond donors toward HO-μ_1 groups. This hydrogen bond induces a significant OH lengthening of the hydrogen bond donor group and a lowering of the stretching frequency: for instance 1.02 Å and 3206 cm^{-1} for a (110) HO-μ_1-Al_{IV} group. During chlorination, the HO-μ_1 group is exchanged into a Cl-μ_1 group with a simultaneous weakening of the hydrogen bond. For the same (110) HO-μ_1-Al_{IV} group, the OH length decreases from 1.02 to 1.00 Å. Its frequency increases from 3206 cm^{-1} to about 3566 cm^{-1}. As a consequence, the weakening of the hydrogen bonds due to the presence of chlorine increases the stretching frequency of some OH groups and explains the broadening of the bands in the 3700−3600 cm^{-1} region.

Pyridine Adsorption. A fruitful comparison of DFT calculations[21] for pyridine adsorption with IR characterization[39] was recently provided for non-chlorinated γ-alumina surfaces. For the chlorine-free surface, it was observed that pyridine molecules adsorb on both Lewis and Brønsted acidic sites; however, the formation of pyridinium ions was not observed. FTIR of pyridine adsorbed on chlorinated γ-alumina revealed that the acidity is increased[40] and that the IR spectrum can exhibit a

(38) Meyer, R. J. *Vib. Spectrosc.* **2007**, *43*, 26.

(39) Morterra, C.; Magnacca, G. *Catal. Today* **1996**, *27*, 497.

(40) Berteau, P.; Kellens, M. A.; Delmon, B. *J. Chem. Soc., Faraday Trans.* **1991**, *87*, 1425.

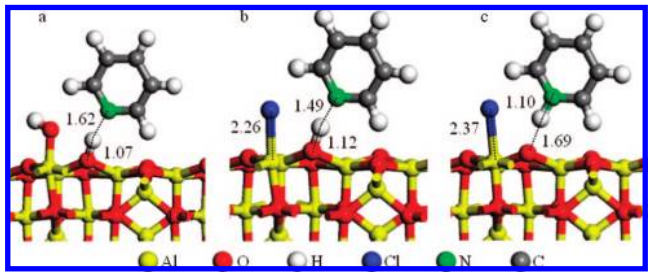

Figure 4. Adsorption of pyridine on the OH-μ_2-Al_{VI} group of the (100) γ-alumina surface: (a) without exchanged chlorine atom on OH-μ_1-Al_{VI}, (b) with exchanged chlorine atom on the μ_1-Al_{VI} group and hydrogen bonded complex, and (c) with exchanged chlorine atom on the μ_1-Al_{VI} group and pyridinium ion formation. The Al−Cl, O−H and N−H distances are quoted in Å.

band at 1540 cm^{-1}, due to the formation of the pyridinium ion.[41] In what follows, our main focus is to explore by DFT simulation how the surface chlorination would influence adsorption of basic probe molecules such as pyridine.

The Brønsted acidity has been studied on the (100) surface for 2.2 OH·nm^{-2} and 2.2 Cl·nm^{-2}. This surface corresponds to the dissociative adsorption of a single HCl molecule. Before chlorination, the surface exhibits one HO-μ_1-Al_{VI} group and one HO-μ_2-Al_{VI} group. The HO-μ_2 is a hydrogen bond donor toward the oxygen atom of the HO-μ_1 groups. For both groups, pyridine adsorbs on hydroxyl groups and forms the O−H···N hydrogen-bonded complex. The exothermic adsorption energy is −15 kJ·mol^{-1} for the HO-μ_2 group (see Figure 4 a). After chlorination, the HO-μ_1-Al_{VI} group is converted into a Cl-μ_1-Al_{VI} group, and the HO-μ_2-Al_{VI} group remains as a Brønsted site. The adsorption energy of pyridine via hydrogen bond on this site (figure 4 b) is strongly enhanced (−50 kJ·mol^{-1}), compared to the non-chlorinated surface (−15 kJ·mol^{-1}). Even if this group remains a hydrogen bond donor, the hydrogen bond O−H···Cl formed with Cl is weaker, compared to the O−H···O before chlorination. This implies that the proton of the O−H group becomes more labile after chlorination. Hence, in presence of pyridine, the stretching of the O−H bond length is increased by +0.05 Å after chlorination. Moreover, by transferring the proton to the nitrogen atom of pyridine, inducing the pyridinium ion formation (Figure 4 c), the adsorption is even more stabilized at −57 kJ·mol^{-1} against −50 kJ·mol^{-1} for hydrogen-bonded complex formation. In line with the IR experiments reported in the literature [40,41] and the OH stretching frequency analysis described in the previous paragraph, the weakening of the hydrogen-bond network by chlorine doping (making the HO-μ_2-Al_{VI} group more available) may be at the origin of the acidity increase as evaluated by pyridine adsorption.

Energy Models of Higher Chlorination Level of γ-Alumina. In the previous paragraphs, we focused on surfaces with low or moderate chlorine content (in the range 1−2 wt %). However, it is well-known that the alumina surface acidity can be enhanced by increasing the chlorine content even more. For instance, the isomerization catalyst requires a strong acid function: the chlorine content can usually reach 8 wt %, whereas for reforming catalysts the chlorine content is around 2 wt %.[4]

It is also known experimentally that the (110) surface of γ-alumina nanocrystallites is predominant (about 70−80% according to[32,33]). Furthermore, as shown in previous paragraphs, it contains the most exchangeable hydroxyl groups in a reasonably high concentration. Hence, to build the DFT thermodynamic model quantifying the surface concentration of chlorine in realistic $p(H_2O)$, $p(HCl)$, and temperature (T) conditions, we will consider only the (110) surface. Chlorine coverages are explored up to 5.9 Cl·nm^{-2}. At this coverage, each aluminum site is bonded to a single chlorine atom.

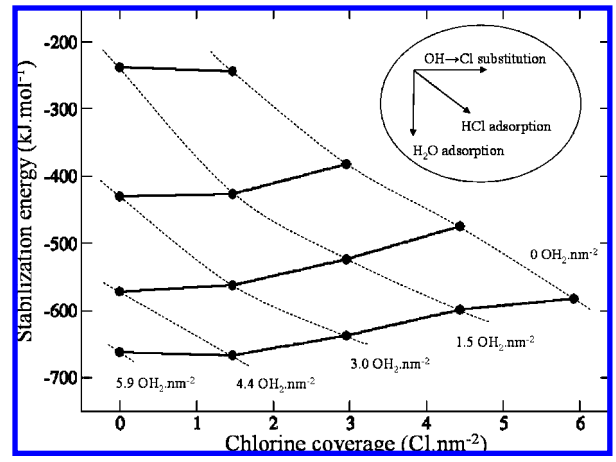

Figure 5. Surface stabilization energy as a function of the chlorine coverage. The dark lines symbolize the iso-total coverage curves (θ_{H_2O} + θ_{HCl} constant) and dashed lines symbolize the iso-water coverage curves (θ_{H_2O} constant). (Insert) Surface mechanisms associated when one moves from one point of the diagram to an adjacent point.

These values of the stabilization energies, E_{stab} and G_{stab}, as defined in the Theoretical Methods section, are reported in Figure 5 for the same partial pressure of H_2O and HCl and the two relevant temperatures used either in isomerization (T = 400 K) or in reforming (T = 800 K).

The following general trends can be pointed out. First, when the total number of adsorbed molecules, *i.e.* the total coverage, increases, the average stabilization energy increases, meaning that the surface tends to saturate the coordination sphere of the Al and O surface atoms. Then, the substitution of the first OH group by one chloride anion can be considered as an athermal process, whatever the total coverage. This result is consistent with the conclusions obtained for the low chloride content surfaces and gives an extrapolation for the larger Cl coverages. When the chlorine amount increases (beyond the chlorine coverage of 1.4 Cl·nm^{-2}), the substitution of OH groups becomes an endothermic process. For a given total coverage, the surface is more and more destabilized when the amount of chloride anions increases due to their increasing lateral repulsive interaction. The *fcc* sublattice of oxygen atoms of γ-alumina exhibits O−O distances between 2.6 and 2.9 Å. In contrast, the reference $AlCl_3$ lamellar material[42] exhibits minimum Cl−Cl distances of 3.1 and 3.3 Å. As a consequence, for large chlorine amounts, the Cl−Cl distances on the surface layer become frustrated, and repulsive anionic interactions destabilize the system. Furthermore, in the case of the hydroxylated surfaces, the lateral interactions of OH groups were partially stabilized by hydrogen bonds. As already shown in the previous paragraphs, the chlorine substitution destabilizes the hydrogen-bond network which also contributes to endothermic energy. Finally, for highly chlorinated alumina, the formation of the $AlCl_3$ phase cannot be excluded. Even if this is beyond the scope of the current work, we suggest that the growth of such a phase would

(41) Clet, G.; Goupil, J. M.; Cornet, D. *Bull. Soc. Chim. Belg.* **1997**, *134*, 223.

(42) Troyanov, S. I. *Russ. J. Inorg. Chem.* **1992**, *37*, 121.

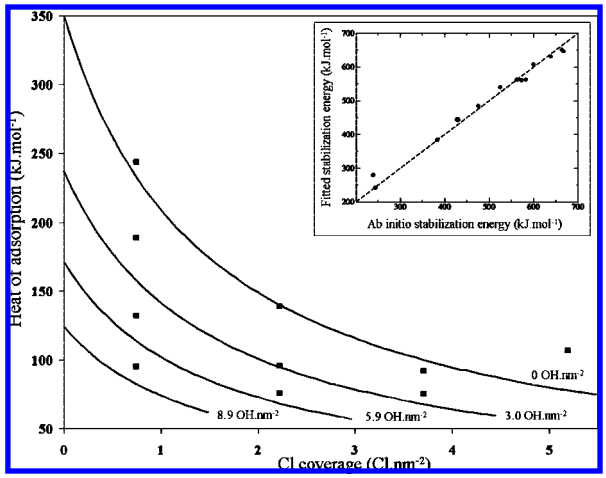

Figure 6. Heat of adsorption of HCl as a function of the Cl surface coverage and for different initial hydroxyl coverage (expressed in $OH \cdot nm^{-2}$). The lines correspond to the analytical expressions derived from eq 7 and the black squares to the ab initio calculated heats of adsorption. (Inset) Ab initio stabilization energy versus the fitted stabilization energy (see the text for parameters).

require a process involving aluminum ion extraction (resulting from strong surface reconstruction) followed by crystallization resulting from combination of Al and Cl into $AlCl_3$.

In order to obtain a continuous description of surface chlorination, instead of discrete values for specific surface coverages, the stabilization energies, reported in the inset of Figure 6, have been fitted using the following analytical expression:

$$E_{stab}(\theta_{H_2O},\theta_{HCl}) = -\alpha \ln(1+A\theta_{H_2O}) - \beta \ln(1+A\theta_{HCl}) + \gamma \ln(1+A\theta_{H_2O}) \ln(1+A\theta_{HCl}) \quad (7)$$

where E_{stab} is the stabilization energy, A the geometric area of the (110) surface model, and α, β, γ are the fitted parameters. Using standard fitting procedures, the following values are obtained: $\alpha = 404$, $\beta = 350$, and $\gamma = 163$ $kJ \cdot mol^{-1}$. As shown in the inset, the correlation is excellent ($R^2 = 0.9907$).

At this stage, it is required to add some comments about the physical interpretation of the proposed analytic expression 7. It is usual in experimental studies on adsorption isotherms to report the heat of absorption of gaseous molecules as a function of the molecular coverage. In our simulation, the heat of adsorption corresponds actually to the derivative of the stabilization energy. Assuming that the surface initially exhibits a known hydroxyl coverage (θ_{H_2O}), the heat of adsorption of hydrogen chlorine on the (100) γ-alumina surface as a function of the Cl surface coverage is given by:

$$\Delta H(\theta_{HCl}) = -\left(\frac{\partial E_{stab}(\theta_{H_2O},\theta_{HCl})}{\partial \theta_{HCl}}\right)_{\theta_{H_2O}} = \frac{\beta - \gamma \ln(1+A\theta_{H_2O})}{1+A\theta_{HCl}} \quad (8)$$

The heat of adsorption for different values of θ_{H_2O} (expressed in $OH \cdot nm^{-2}$) is plotted in Figure 6, evidencing the strong impact of the initial hydroxyl coverage on the HCl adsorption isotherm. For the low HCl coverage limit, the heat of adsorption can be expressed as:

$$\Delta H(\theta_{HCl}) \approx \Delta H^0(\theta_{H_2O})(1 - \alpha_T \theta_{HCl}) \quad (9)$$

Hence, this expression corresponds to a Tempkin−Frumkin adsorption isotherm type,[43,44] which assumes that the heat of adsorption decreases linearly with coverage due to adsorbate/adsorbate interactions. α_T is a fitting parameter, and ΔH^0 is the initial heat of adsorption which decreases when the initial hydroxyl coverage increases: from 350 $kJ \cdot mol^{-1}$ for a hydroxyl-free surface to 124 $kJ \cdot mol^{-1}$ for a surface with 8.9 $OH \cdot nm^{-2}$. Our results show that a linear Tempkin-type of adsorption isotherm would only be approximate and would not take into the attractive hydrogen bonds (OH···Cl) compensating the repulsive adsorbate−adsorbate interaction.

Hydroxyl and Chlorine Surface Concentrations in Reaction Conditions. This analytical expression, combined with the equation of stabilization energy (eq 7) is used to determine the stable surface termination and the species surface concentration as a function of temperature and hydrogen chloride and water partial pressures. Two partial water pressures relevant for the reforming and isomerization processes have been considered: $P_{H_2O} = 1$ and $P_{H_2O} = 0.001$ bar (Figures 7 and 8). Concerning surface hydroxyls (Figure 7), low temperatures favor high surface concentration. The effect of HCl partial pressure on the OH concentration depends on the water pressure and temperature. In wet atmospheres ($P_{H_2O} = 1$ bar and T below 600 K), the OH concentration remains roughly constant whatever the HCl partial pressures (except very high HCl partial pressure), whereas for low water pressure ($P_{H_2O} = 0.001$ bar), the concentration increases with increasing HCl partial pressure as a result of HCl dissociative adsorption on Al and O free sites. Nevertheless, the order of magnitude is not drastically different for the two cases. This means that the number of potential Brønsted acid sites is relatively stable, whatever the water content. As shown in the previous section, the acid strength of theses sites strongly depends on the chlorine content. Concerning the chlorine concentration, the comparison between the two water partial pressures demonstrates the strong impact of residual water on chlorine coverage (Figure 8). For $P_{H_2O} = 1$ bar, it is impossible to obtain high chlorine coverage, even for low temperature and high HCl partial pressure. For $P_{H_2O} = 0.001$ bar, high chlorine coverage (>3 $Cl \cdot nm^{-2}$) can be achieved even at 800 K.

Impact for the Reforming and Isomerization Processes. The catalysts for reforming are always derived from platinum deposited on chlorinated alumina. Chlorine is added to promote the acid function of alumina. The chlorine content is usually close to 1 wt %, and the operating temperatures are between 750 and 820 K. The chlorine contents (expressed in wt %) of the alumina support and assuming a specific area of 200 $m^2 \cdot g^{-1}$, have been calculated as a function of HCl partial pressure and for an average temperature of 800 K (Figure 9). At this temperature, for water partial pressures between 0.001 and 1 bar, the differences of chlorine contents remain moderate and roughly constant when the HCl partial pressures increase (approximately 1 Cl wt %). If the contacting gas is correctly dried, the 1 Cl wt % target is reached, even for low HCl content.

Platinum deposited on chlorinated γ-Al_2O_3 is also industrially used as catalyst for light paraffin isomerization. In this case, the acidic function of the catalyst must be enhanced by increasing the chlorine content of the industrial catalyst which comprises between 5 and 12 wt %. The isomerization reactions are performed at low temperature, which comprises between 390 and 450 K.[4] The chlorine content has been calculated for a temperature of 400 K (Figure 9).

(43) Slygin, A.; Frumkin, P. *Acta Physiochim. URSS* **1935**, *3*, 791.
(44) Tempkin, M. I.; Pyshev, V. *Acta Physiochim. URSS* **1940**, *69*, 217.

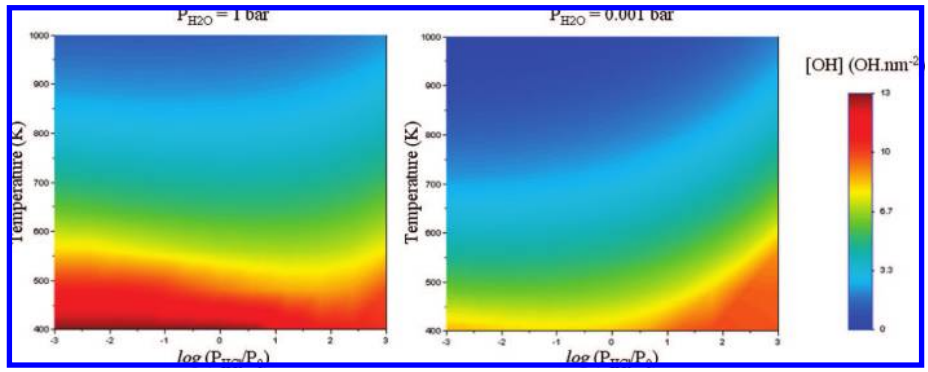

Figure 7. Hydroxyl coverage, in OH·nm^{-2}, as a function of temperature and hydrogen chloride partial pressure for $P_{H_2O} = 1$ bar and $P_{H_2O} = 0.001$ bar.

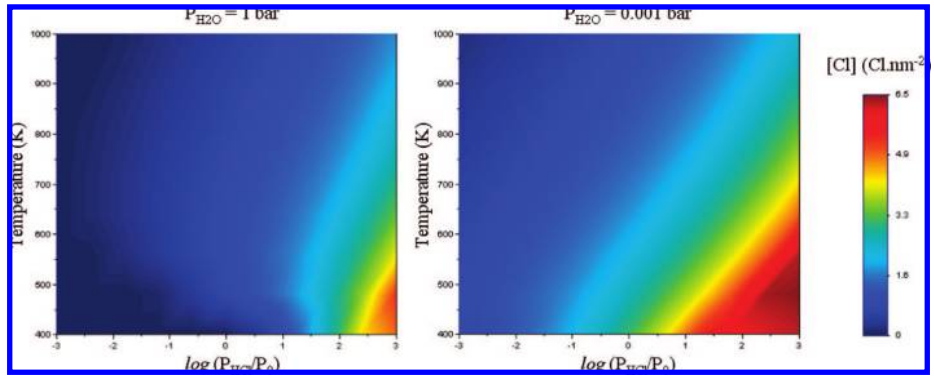

Figure 8. Chlorine coverage, in Cl·nm^{-2}, as a function of temperature and hydrogen chloride partial pressure for $P_{H_2O} = 1$ bar and $P_{H_2O} = 0.001$ bar.

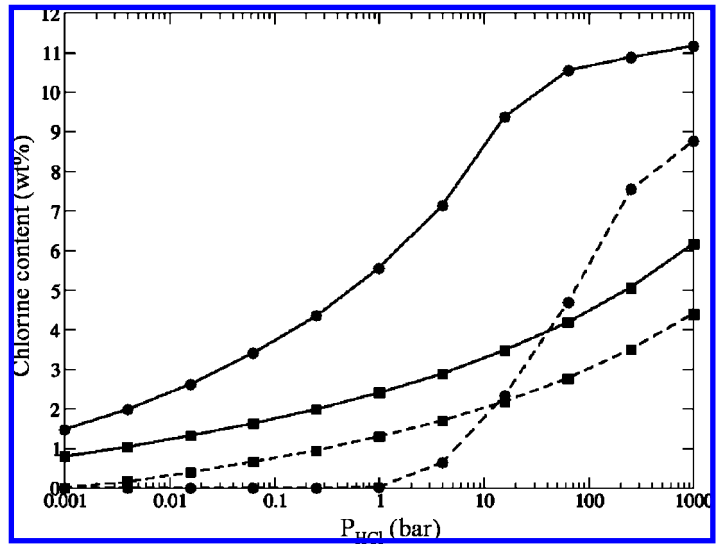

Figure 9. Chlorine content of γ-alumina (expressed in wt %, assuming a specific area of 200 m^2·g^{-1}) as a function of hydrogen chlorine partial pressure for different conditions: for low residual water content ($P_{H_2O} = 0.001$ bar, full line) and for high residual water level ($P_{H_2O} = 1$ bar, dotted line), for $T =$ 400 K (circles) and $T = 800$ K (squares).

Compared to the reforming case, the residual water content has a drastic impact on the chlorine content: for low temperature, the difference between a dry and a wet atmosphere can be as large as 6 Cl wt %. For moderate HCl partial pressure, the chlorine content required for isomerization can only be reached for dry atmospheres ($P_{H_2O} = 0.001$ bar).

The thermodynamic model constructed from DFT calculations of HCl and H_2O coadsorption isotherms renders coherent and quantitative trends in surface species distribution for two industrial supports. The interpretation of the effect of temperature and partial pressures is crucial for an optimal control of the surface state of γ-alumina in industrial conditions.

Mechanisms of Surface Chlorination. In what follows we address the open question of surface chlorination mechanisms, often discussed in literature. Indeed, gaseous HCl molecules can react with the surface through the exchange of one Al−OH group by one Al−Cl group with the release of one water molecule (eq 1). A second chemical scenario is the dissociative adsorption of the HCl molecule on free Al sites adjacent to O sites, leading to the formation of new Al−Cl and Al−OH

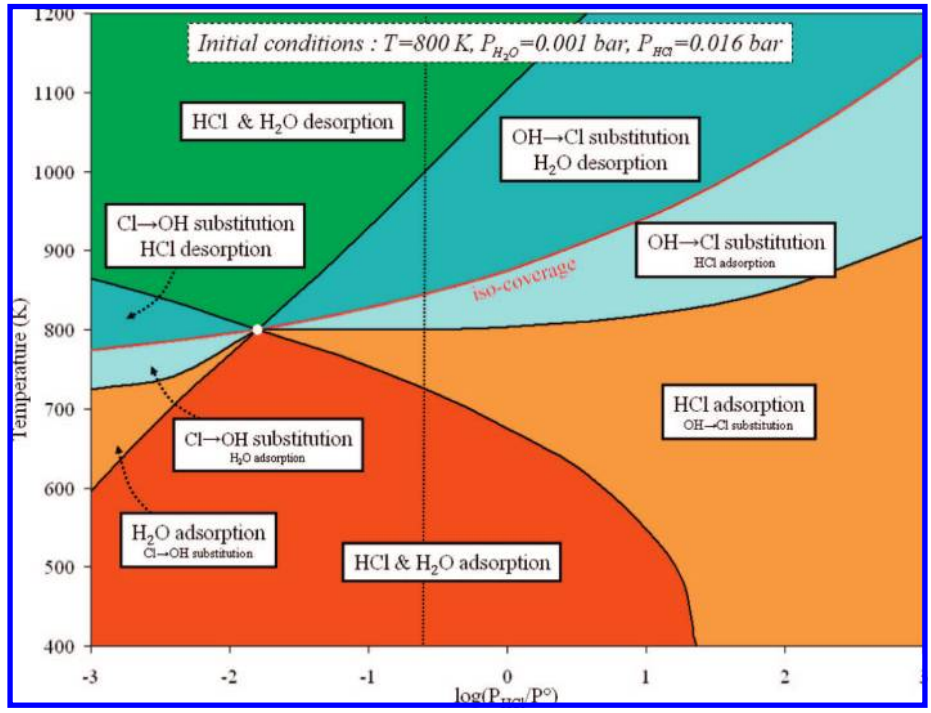

Figure 10. Mechanisms of surface evolution of the (100) γ-alumina surface as a function of the final temperature and HCl pressure (at fixed P_{H_2O} equal to 0.001 bar). The diagram assumes that the initial surface corresponds to the stable termination for $T = 800$ K, and $P_{HCl} = 0.016$ bar (see text for explanations). The vertical dashed line corresponds to $P(HCl) = 0.25$ bar.

surface groups. In the latter case, the appearance of new OH groups, as observed by IR spectroscopic studies by some authors,[45,46] supports the dissociative adsorption mechanism. In the former case, other authors have shown that, in some experimental conditions, the equilibrium chlorine content as a function the H_2O/HCl molar ratio can be interpreted, assuming that only exchanges between OH and Cl surface groups are involved.[37] Moreover, by combining FTIR and ^{1}H MAS NMR it has been found that the exchange reaction occurs whatever the experimental conditions and that the adsorption mechanism becomes significant when the reaction temperature decreases.[47] More recently, by applying IR spectroscopy, TPD, and inelastic neutron scattering spectroscopy for η-alumina,[48] the existence of both mechanisms has been confirmed and correlated to the nature of the Lewis acid site. Using the previously established stability diagrams of OH and Cl species on the (110) surface, it is possible to also obtain insights about the mechanisms of surface chlorination. The nature of the involved mechanisms is strongly dependent on the initial and final conditions (temperature, water and hydrogen chlorine pressures) that are considered. As these mechanisms are crucial for the reforming process, we consider the stable termination of the (110) γ-alumina surface close to 800 K, with $P_{H_2O} = 0.001$ bar and$P_{HCl} = 0.016$ bar ($\theta_{H_2O} = 1.0$ $H_2O \cdot nm^{-2}$ and $\theta_{HCl} = 0.7$ $HCl \cdot nm^{-2}$) as the starting conditions used in typical reforming units. The different domains of surface evolution as a function of the final temperature and HCl pressure (the water pressure remaining constant) are reported in Figure 10. For a given temperature, a single HCl pressure allows to keep the total coverage ($\theta_{H_2O} + \theta_{HCl}$) equal to 1.7 $(H_2O+HCl) \cdot nm^{-2}$. This iso-coverage curve is represented by the red curve in Figure 10. Along this curve, the substitution is the only possible mechanism: OH→Cl for $P_{HCl} > 0.016$ bar and Cl→OH for $P_{HCl} < 0.016$ bar. As qualitatively expected, when the HCl partial pressure increases (respectively decreases), the total pressure increases (respectively decreases); thus, the temperature must be increased (respectively decreased), if one wishes to maintain the total coverage constant. For temperatures higher than the iso-coverage temperature, the total coverage tends to decrease. For instance, if the final HCl pressure is equal to 0.25 bar (log ($P_{HCl}/P°$) = −0.6), the iso-coverage temperature is about 845 K. For final temperatures between 845 and 1000 K, water molecules will desorb and some OH surface groups will be substituted by Cl surface groups. As a consequence, the surface is chlorine-enriched, and the total coverage decreases, leading to the formation of surface unsaturated groups. For final temperatures higher than 1000 K, both HCl and H_2O molecules will desorb. For temperatures lower than the iso-coverage temperature, the total coverage tends to increase. Keeping the same example (log ($P_{HCl}/P°$) = −0.6), for temperatures lower than 845 K, the surface will be chlorine-enriched. For temperatures between 725 and 845 K, OH→Cl substitution and HCl dissociative absorption will occur simultaneously: for temperature higher than 800 K, the substitution is the predominant mechanism. For temperature lower than 725 K, the absorption of both HCl and H_2O molecules will occur, leading to the progressive saturation of coordinately unsaturated surface sites. Similar results can be obtained for final HCl pressures lower than the initial HCl pressure (0.016 bar): the chlorine surface content will tend to decrease. As a conclusion, the nature of the mechanism involved during surface chlorination is complex and is strongly affected by the initial and final thermodynamic

(45) Peri, J. B. *J. Phys. Chem.* **1966**, *70*, 1483.
(46) Tanaka, M.; Ogasawara, S. *J. Catal.* **1970**, *16*, 157.
(47) Kytökivi, A.; Lindblad, M.; Root, A. *J. Chem. Soc., Faraday Trans.* **1995**, *91*, 941.
(48) McInroy, A. R.; Lundie, D. T.; Winfield, J. M.; Dudman, C. C.; Jones, P.; Parker, S. F.; Lennon, D. *Catal. Today* **2006**, *114*, 403.

conditions. The pure substitution of Cl and OH surface groups can only be obtained for a limited set of experimental conditions.

Conclusions

This DFT study of chlorinated γ-alumina surfaces has revealed new concepts for the chemical process involved in chlorination of γ-alumina surfaces in various conditions of temperature and partial pressures of water and HCl as found at laboratory- and industrial-scale processes (catalytic isomerization and reforming). At the laboratory scale and low chlorine contents, the combination of DFT calculations of vibrational frequencies of hydroxyl groups and IR spectroscopy has revealed that the most basic μ_1-OH groups present on the (100) and (110) surfaces are preferentially exchanged. The weakening of the hydrogen-bond network after chlorination has been found to play a key role in the change of surface Brønsted acidity. As simulated by pyridine adsorption, the formation of the pyridinium ion on μ_2-OH sites was favored after chlorine exchange, due to the loss of the hydrogen bond of the μ_2-OH species with the neighboring basic μ_1-OH groups once exchanged by Cl.

For higher chlorination contents as industrially used in isomerization or reforming conditions, we have determined numerous configurations of adsorbed and exchanged chlorine on γ-alumina surfaces with various hydration degrees. The competitive effects of water and HCl partial pressures were thus put forward, thanks to a thermodynamic model including DFT values of total energies and the chemical potential of the two reactants. When considering a morphology model for γ-alumina nanoparticles, this approach has led to the quantitative evaluation of chlorine content as a function of partial pressures of HCl and temperature. For a temperature close to isomerization, the value of chlorine content can reach up to 6% chlorine, whereas for the temperature used in reforming, the chlorine content is limited to upper values of 2% for realistic HCl partial pressures. These quantitative insights are crucial for a better control of the chemical balance between water and chlorine surface concentration on the catalytic support. Furthermore, depending on the reaction conditions and on the initial thermodynamical state of the surface, our study has determined the different domains of the chlorination mechanisms (substitution process versus dissociative addition process).

Our model approach provides new insights in the competition between H_2O and HCl on a γ-alumina surface and on the influence of Cl groups on the acidity of the remaining hydroxyls. The combination between a thermodynamic model and DFT total energy calculations is hence a powerful tool to map the various regimes of adsorption and substitution for these two molecules, and therefore to obtain a predictive model of the surface chemical properties in the temperature and pressure conditions used in the experiment. We hope that these new structural models of the chlorinated alumina surfaces can deserve future theoretical and experimental investigations of the reactivity on Cl-γ-alumina-supported metal particles such as those used in reforming catalysis.

Acknowledgment. Part of this work was undertaken within the Groupement de Recherche Européen "Dynamique Moléculaire Quantique Appliquée à la Catalyse", a joint project of IFP-CNRS-TOTAL-Universität Wien. We thank the Institut du Développement et des Ressources en Informatique Scientifique (IDRIS) for providing computational resources. M.D. and P.R. thank P. Euzen and P.-Y. Le Goff from Axens for fruitful discussions on the industrial reforming process.

JA8019593